

# Differential blockade of neuronal voltage-gated Na<sup>+</sup> and K<sup>+</sup> channels by antidepressant drugs

Graham M. Nicholson\*, Tim Blanche<sup>1</sup>, Kylie Mansfield<sup>2</sup>, Yvonne Tran

Department of Health Sciences, University of Technology, P.O. Box 123, Sydney, Broadway NSW 2007, Australia

Received 7 August 2002; accepted 9 August 2002

## Abstract

The effects of a range of antidepressants were investigated on neuronal voltage-gated Na<sup>+</sup> and K<sup>+</sup> channels. With the exception of phenelzine, all antidepressants inhibited batrachotoxin-stimulated <sup>22</sup>Na<sup>+</sup> uptake, most likely via negative allosteric inhibition of batrachotoxin binding to neurotoxin receptor site-2 on the Na<sup>+</sup> channel. Imipramine also produced a differential action on macroscopic Na<sup>+</sup> and K<sup>+</sup> channel currents in acutely dissociated rat dorsal root ganglion neurons. Imipramine produced a use-dependent block of Na<sup>+</sup> channels. In addition, there was a hyperpolarizing shift in the voltage-dependence of steady-state Na<sup>+</sup> channel inactivation and slowed repriming kinetics consistent with imipramine having a higher affinity for the inactivated state of the Na<sup>+</sup> channel. At higher concentrations, imipramine also blocked delayed-rectifier and transient outward K<sup>+</sup> currents in the absence of alterations to the voltage-dependence of activation or the kinetics of inactivation. These actions on voltage-gated ion channels may underlie the therapeutic and toxic effects of these drugs.

© 2002 Elsevier Science B.V. All rights reserved.

**Keywords:** Na<sup>+</sup> channel; K<sup>+</sup> channel; Antidepressant; Imipramine; Patch clamping; <sup>22</sup>Na<sup>+</sup> flux

## 1. Introduction

Antidepressants are effective in the management of depression, obsessive compulsive disorder, and enuresis. In addition, they also provide analgesia for a variety of neuropathic and headache pain syndromes, regardless of the presence of depression (Richeimer et al., 1997). Unfortunately, they are associated with numerous undesirable side-effects, including sedation, which complicate their use in the long-term management of these disorders. The most serious of these is the propensity of certain antidepressants to induce cardiac arrhythmias, characterized by quinidine-like direct membrane effects in the heart and epileptic-like seizures (reviewed by Rosenstein et al., 1993).

Whilst the molecular mechanism by which antidepressants induce sedation, seizures and arrhythmias appears not to involve their therapeutic actions to enhance monoamine

transmission (Trimble, 1980), it remains unclear whether modulation of ion channel function is involved. Several studies of the effects of antidepressants on voltage-gated ion channels have been undertaken. In cardiac tissue, extensive electrophysiological studies of imipramine have shown that it blocks cardiac Na<sup>+</sup> currents in a voltage- and use-dependent manner similar to lidocaine, flecainide and quinidine (Vaughan Williams, 1984; Bou-Abboud and Nattel, 1998) resulting in imipramine being classified as a class Ia or intermediate kinetics antiarrhythmic drug (Delpón et al., 1990). In neuronal tissues, the tricyclic antidepressant drug amitriptyline has also been shown to inhibit Ca<sup>2+</sup>-activated K<sup>+</sup> channels, including both the large conductance (*I*<sub>BK(Ca)</sub>) (Lee et al., 1997) and small conductance (*I*<sub>SK(Ca)</sub>) subtypes (Grunnet et al., 2001). Moreover, previous studies of imipramine in neuronal tissue have shown that it also blocks voltage-gated Na<sup>+</sup>, K<sup>+</sup> and Ca<sup>2+</sup> currents in neuroblastomas (Ogata and Narahashi, 1989) and certain K<sup>+</sup> currents in sympathetic (Wooltorton and Mathie, 1995) neurons. However, in many cases the electrophysiological properties or the specificity of neuronal block of these voltage-gated ion channels was not well characterized.

In addition to the lack of detailed analyses of antidepressant action on Na<sup>+</sup> currents there is only limited neurochemical studies on the site(s) of action of these drugs. A

\* Corresponding author. Tel.: +61-2-9514-2230; fax: +61-2-9514-2228.

E-mail address: Graham.Nicholson@uts.edu.au (G.M. Nicholson).

<sup>1</sup> Present address: Department of Ophthalmology, University of British Columbia, 2550 Willow Street, Vancouver, BC, Canada V5Z 3N9.

<sup>2</sup> Present address: Department of Physiology and Pharmacology, University of New South Wales, NSW 2052, Australia.

previous study has shown that tricyclic and tetracyclic antidepressants inhibit veratridine-activated  $^{22}\text{Na}^+$  flux in adrenal medullary cells (Arita et al., 1987), but it is not known to which of the seven orphan receptor sites on the  $\text{Na}^+$  channel they may interact (for a review of the neurotoxin receptor sites, see Gordon, 1997). Nevertheless, several other drugs, including lidocaine and the anticonvulsants phenytoin and carbamazepine, have been shown to cause an indirect negative allosteric interaction with neurotoxin receptor site-2 but fail to interact with neurotoxin receptor site-1 (Willow and Catterall, 1982).

The principal objective of this study was to examine the effects of antidepressants on a variety of voltage-gated  $\text{Na}^+$  channel subtypes in neuronal membranes, using a combination of  $^{22}\text{Na}^+$  uptake, radiolabelled neurotoxin receptor binding and patch clamp techniques. In addition, we examined the effects of antidepressants on specific subtypes of  $\text{K}^+$  channels given their significant role in neuronal depolarization and regulation of excitability. Moreover, we have given careful consideration to a comparison of the concentration dependence of any drug actions with in vivo tissue levels of antidepressant drugs.

## 2. Materials and methods

### 2.1. Preparation of rat brain synaptosomes

Synaptosomes for  $^{22}\text{Na}^+$  uptake and radiolabelled neurotoxin binding assays were prepared from the brains of male Wistar rats (4–8 weeks, 250–350 g) using a combination of homogenization and differential density gradient centrifugation according to the method described previously (Little et al., 1998b). Synaptosomes were suspended in a solution consisting of (mM): choline Cl 130, KCl 5.4,  $\text{MgSO}_4$  0.8, D-glucose 5.5 and HEPES–Tris 50 (pH 7.4, 37 °C), and were stored in liquid nitrogen until required. Membrane protein concentration was determined using a Bio-Rad protein assay with bovine serum albumin as a standard.

### 2.2. $^{22}\text{Na}^+$ uptake assays

The effect of antidepressants on  $^{22}\text{Na}^+$  uptake in rat brain synaptosomes was determined using the method described previously (Little et al., 1998b). Briefly, rat brain synaptosomes (500  $\mu\text{g}$  membrane protein) were preincubated for 30 min with toxins in 100  $\mu\text{l}$  of  $\text{Na}^{2+}$ -free medium at 37 °C. The preincubation medium contained (mM): choline Cl 130, KCl 5.4,  $\text{MgSO}_4$  0.8, D-glucose 5.5, HEPES–Tris 50 (pH 7.4, 37 °C) and 1 mg/ml bovine serum albumin. Uptake was initiated by adding 150  $\mu\text{l}$  of assay medium containing (mM): choline Cl 128, KCl 5.4,  $\text{MgSO}_4$  0.8, D-glucose 5.5, HEPES–Tris 50 (pH 7.4, 37 °C), NaCl 2.66, ouabain 5, 1 mg/ml bovine serum albumin and 0.9  $\mu\text{Ci/ml}$  of carrier-free  $^{22}\text{NaCl}$  (Du Pont, Boston, MA, USA). After 5 s, uptake was terminated by the addition

of 4 ml of ice-cold wash solution and rapid filtration through 0.45- $\mu\text{m}$  nitrocellulose membrane filter (Millipore, Sydney, Australia). The wash solution consisted of (mM): choline Cl 163,  $\text{CaCl}_2$  1.8,  $\text{MgSO}_4$  0.8, HEPES–Tris 5 (pH 7.4, 4 °C) and 1 mg/ml bovine serum albumin. The filter discs were washed twice further with 4 ml of wash solution. Maximal  $^{22}\text{Na}^+$  uptake was determined in the presence of 1  $\mu\text{M}$  batrachotoxin whilst uptake not mediated by voltage-gated  $\text{Na}^+$  channels was determined in the presence of 1  $\mu\text{M}$  tetrodotoxin (Calbiochem, Alexandria, NSW, Australia). Non-specific  $^{22}\text{Na}^+$  uptake was typically less than 35% of total uptake.

### 2.3. Radiolabelled neurotoxin-binding assays

Equilibrium competition binding assays were performed using increasing concentrations of the antidepressants in the presence of a constant low concentration of the radiolabelled toxin. [ $^3\text{H}$ ]saxitoxin ([ $^3\text{H}$ ]STX) binding assays were performed using the method described previously (Little et al., 1998a). Briefly, rat brain synaptosomes (300  $\mu\text{g}$ ) were suspended in 0.2 ml buffer and 2 nM [ $^3\text{H}$ ]STX (0.2  $\mu\text{Ci}$ ; Amersham, Little Chalfont, Buckinghamshire, England). After incubation for 30 min at 37 °C the reaction was terminated by the addition of 4-ml ice-cold wash buffer and filtered through Whatman GF/B glass-fibre filters. Filters were then washed twice with 4 ml of wash solution. Non-specific binding was determined in the presence of 1  $\mu\text{M}$  tetrodotoxin and was typically 5–15% of total binding. [ $^3\text{H}$ ]batrachotoxin A-20 $\alpha$ -benzoate ([ $^3\text{H}$ ]BTX) binding experiments were performed according to the method described by Little et al. (1998b). Rat brain synaptosomes (350  $\mu\text{g}$  protein/ml) were suspended in 0.2 ml buffer, containing 0.3  $\mu\text{M}$  scorpion  $\alpha$ -toxin ( $\alpha$ -LqqV), 1  $\mu\text{M}$  tetrodotoxin and 10 nM [ $^3\text{H}$ ]BTX (0.6  $\mu\text{Ci}$ ; Du Pont).  $\alpha$ -LqqV was purified from the venom of the scorpion *Leiurus quinquestriatus quinquestriatus* using ion-exchange chromatography according to the method of Catterall (1976) and used to allosterically enhance the affinity of [ $^3\text{H}$ ]BTX binding. After incubation for 30 min at 37 °C, the reaction mixture was diluted with 4-ml ice-cold wash solution and separation of free from bound toxin was achieved by rapid filtration under vacuum through Whatman GF/C glass-fibre filters. Non-specific binding was determined in the presence of 300  $\mu\text{M}$  veratridine (Sigma, St. Louis, MO, USA) and was typically 5–15% of total binding.

### 2.4. Electrophysiological recordings

All electrophysiological experiments were conducted on acutely cultured dorsal root ganglia neurons dissociated from 4- to 12-day-old Wistar rats as described previously (Nicholson et al., 1994). Voltage-gated  $\text{Na}^+$  current ( $I_{\text{Na}}$ ) or  $\text{K}^+$  currents ( $I_{\text{K}}$ ) were recorded using the whole-cell configuration of the patch-clamp technique. Micropipettes were pulled from borosilicate glass-capillary tubing and had d.c. resis-

tances of 0.8–1.5 M $\Omega$  for recording  $I_{\text{Na}}$  or 1–2.5 M $\Omega$  for recording  $I_{\text{K}}$ .

The recording solutions were designed to separate either  $I_{\text{Na}}$  or  $I_{\text{K}}$  from other membrane currents. The internal (pipette-filling) and external solutions for  $I_{\text{Na}}$  were as follows (mM): internal, CsF 135, NaCl 10, HEPES 5, with the pH adjusted to 7.0 with 1 M CsOH; external, NaCl 30, CsCl 5, KCl 5, CaCl<sub>2</sub> 1.8, MgCl<sub>2</sub> 1, D-glucose 25, HEPES 5, tetramethylammonium chloride 70 and tetraethylammonium chloride 20, with the pH adjusted to 7.4 with 1 M tetraethylammonium hydroxide. A low external Na<sup>+</sup> concentration was chosen to improve series resistance compensation and avoid amplifier saturation (Ogata et al., 1989a). The predominant Na<sup>+</sup> channel subtype present in each cell was determined using a modified steady-state Na<sup>+</sup> channel inactivation voltage protocol taking advantage of the separation of steady-state inactivation curves for tetrodotoxin-sensitive and tetrodotoxin-resistant Na<sup>+</sup> channels (for detailed methodology, see Rash et al., 2000). Only those cells which exhibited less than 10% tetrodotoxin-resistant  $I_{\text{Na}}$ , as determined from differences in this steady-state Na<sup>+</sup> channel inactivation profile, were used to determine the actions of toxins on tetrodotoxin-sensitive  $I_{\text{Na}}$ . To isolate tetrodotoxin-resistant  $I_{\text{Na}}$ , 200 nM tetrodotoxin was added to the external solution to block tetrodotoxin-sensitive  $I_{\text{Na}}$ .

The solutions used for experiments on  $I_{\text{K}}$  were as follows (mM): internal, KF 80, tetramethylammonium chloride 50, D-glucose 5, EDTA 5 and HEPES 5, with the pH adjusted to 7.0 using 1 M KOH; external, tetramethylammonium chloride 120, KCl 5, CaCl<sub>2</sub> 1.8 MgCl<sub>2</sub> 1, D-Glucose 25 and HEPES 5, with the pH adjusted to 7.4 using 1 M NaOH. When recording  $I_{\text{K}}$ , 200 nM tetrodotoxin was added to the external solution to block tetrodotoxin-sensitive  $I_{\text{Na}}$ . Cells displaying tetrodotoxin-resistant  $I_{\text{Na}}$  were not used for experiments investigating actions on  $I_{\text{K}}$ . Since Na<sup>+</sup> was absent from the external solution any involvement of Na<sup>+</sup>-dependent  $I_{\text{K}}$  was eliminated. In addition, the internal solution contained 80 mM KF eliminating any Ca<sup>2+</sup>-dependent components of  $I_{\text{K}}$ . To record delayed-rectifier K<sup>+</sup> currents ( $I_{\text{K(DR)}}$ ), 1 mM 4-aminopyridine was added to the external solution to eliminate any possible contamination by transient ('A'-type) outward K<sup>+</sup> currents ( $I_{\text{T}}$ ). This required readjustment of the pH to 7.4 using 1 M HCl. For recordings of  $I_{\text{T}}$ , 25 mM tetraethylammonium chloride was added to the external solution to block  $I_{\text{K(DR)}}$ . Inward-rectifier K<sup>+</sup> currents ( $I_{\text{K(IR)}}$ ) were recorded in 50 mM external KCl and 75 mM external tetramethylammonium chloride.

The osmolarity of the external and internal solutions was adjusted to 300 mosM/l with sucrose to reduce osmotic stress on the dorsal root ganglion cells. Bath temperature was maintained at either 16 or 22 °C by an in-line Peltier cooling device, and did not fluctuate more than 0.2 °C during the course of an experiment.

Stimulation and recording were both controlled by an AxoData© data acquisition system (Axon Instruments, Foster City, CA, USA). Data were filtered using an internal four-

pole 5-kHz Bessel lowpass filter for  $I_{\text{Na}}$  and a four-pole 1-kHz Bessel lowpass filter for  $I_{\text{K}}$ . Digital sampling rates were between 15 and 25 kHz depending on voltage protocol length. Leakage and capacitive currents were digitally subtracted with  $P - P/4$  procedures and series resistance compensation was >80% for all cells. The experiments used in this study were rejected if there were large leak currents or currents showed signs of inadequate space clamping such as an abrupt activation of currents upon relatively small depolarizing pulses.

All animal experimentation was approved by the joint animal ethics committee of the University of Technology, Sydney (UTS), and the Royal North Shore Hospital, Sydney, Australia.

## 2.5. Data analysis

Numerical data are expressed as the mean  $\pm$  S.E ( $n$ , number of observations) and statistical differences were determined using a paired Student's  $t$ -test at  $P < 0.05$ . Mathematical curve-fitting was accomplished using SigmaPlot v4.14 for Macintosh. All curve-fitting routines used a non-linear least-squares method and splining routines.

Concentration–response curves were fitted using the following form of the Logistic equation:

$$y = \frac{1}{1 + ([C]/K_d)^{n_H}} \quad (1)$$

where  $[C]$  is the antidepressant concentration,  $n_H$  is the Hill coefficient (slope parameter), and  $K_d$  is the apparent dissociation constant. The IC<sub>50</sub> values obtained for inhibition of batrachotoxin-stimulated <sup>22</sup>Na<sup>+</sup> and [<sup>3</sup>H]BTX binding were converted to  $K_i$  values according to the relationship described by Cheng and Prusoff (1973).

The fitted curves for the  $I/V$  relationships were obtained using the following equation:

$$I_{\text{Na}} = g_{\text{max}} \left( 1 - \left( \frac{1}{1 + \exp[(V - V_{1/2})/s]} \right) \right) (V - V_{\text{rev}}) \quad (2)$$

where  $I_{\text{Na}}$  is the amplitude of the peak  $I_{\text{Na}}$  at a given test potential,  $V$ ,  $g_{\text{max}}$  is the maximal Na<sup>+</sup> conductance,  $V_{1/2}$  is the voltage at half-maximal activation,  $s$  is the slope factor and  $V_{\text{rev}}$  is the reversal potential.

The values for Na<sup>+</sup> conductance ( $g_{\text{Na}}$ ) and K<sup>+</sup> conductance ( $g_{\text{K}}$ ) were calculated according to the equation:

$$g = \frac{I}{(V - V_{\text{rev}})} \quad (3)$$

The values of  $g_{\text{Na}}$  or  $g_{\text{K}}$  were then normalized against  $g_{\text{max}}$  and fitted to a Boltzmann distribution according to the equation.

$$\frac{g}{g_{\text{max}}} = \frac{1}{1 + [(V_{1/2} - V)/s]} \quad (4)$$

The fitted curves for steady-state  $I_{\text{Na}}$  inactivation ( $h_{\infty}$ ) were obtained using the following form of the Boltzmann equation:

$$h_{\infty} = \frac{1}{1 + [(V - V_{1/2})/k]} \quad (5)$$

where  $V_{1/2}$  is the voltage at half inactivation, and  $k$  is the slope factor.

Curve fitting routines for the unrecovered fraction used to assess the rate of recovery from  $I_{\text{Na}}$  inactivation were obtained using the following double exponential decay function:

$$1 - \frac{I_{\text{test}}}{I_{\text{cond}}} = A \exp(-t/\tau_f) + B \exp(-t/\tau_s) \quad (6)$$

where  $I_{\text{test}}$  is the peak  $I_{\text{Na}}$  during the test pulse,  $I_{\text{cond}}$  is the peak current during the conditioning prepulse,  $\tau_f$  and  $\tau_s$  are the time constants of fast and slow recovery from inactivation, respectively, and  $A$  and  $B$  are the fractions of recovery described by  $\tau_f$  and  $\tau_s$ , respectively.

### 3. Results

#### 3.1. Inhibition of batrachotoxin-stimulated $^{22}\text{Na}^+$ Flux

Initial  $^{22}\text{Na}^+$  flux experiments aimed to establish whether antidepressant drugs were capable of directly activating voltage-gated  $\text{Na}^+$  channels. All antidepressants tested showed no intrinsic ability to activate  $^{22}\text{Na}^+$  flux in synaptosomal  $\text{Na}^+$  channels at concentrations up to 100  $\mu\text{M}$  (Fig. 1A). This indicates that antidepressants do not act as either partial or full agonists to activate  $\text{Na}^+$  channels. We therefore examined the effects of antidepressants on batrachotoxin-stimulated  $^{22}\text{Na}^+$  uptake. Imipramine and amitriptyline (tricyclic non-specific catecholamine reuptake inhibitors), and maprotiline (heterocyclic noradrenaline-selective reuptake inhibitor) were found to produce a concentration-dependent inhibition of batrachotoxin-stimulated  $^{22}\text{Na}^+$  uptake in rat brain synaptosomes (Fig. 1B). Imipramine and amitriptyline inhibited  $^{22}\text{Na}^+$  uptake with respective  $K_i$  values of  $11.3 \pm 1.1 \mu\text{M}$  ( $n=5$ ) and  $10.6 \pm 1.7 \mu\text{M}$  ( $n=3$ ) (Fig. 1B), whilst maprotiline inhibited the uptake with a  $K_i$  value of  $18.7 \pm 2.1 \mu\text{M}$  ( $n=3$ ), respectively (Fig. 1C). In contrast, the hydrazide irreversible monoamine oxidase inhibitor, phenelzine (Fig. 1C), showed little inhibition of batrachotoxin-stimulated  $^{22}\text{Na}^+$  uptake ( $n=4$ ). Even at 1 mM, several orders of magnitude higher than would be present at therapeutic doses, only partial inhibition of flux was observed.

#### 3.2. Binding assays

It is well known that saxitoxin and tetrodotoxin act to inhibit the influx of  $\text{Na}^+$  through voltage-gated  $\text{Na}^+$  chan-

nels by binding to neurotoxin receptor site-1 at the mouth of the channel pore (Gordon, 1997). The possibility that inhibition of  $^{22}\text{Na}^+$  uptake by antidepressant drugs could be mediated by a similar mechanism was investigated by competitive binding experiments with [ $^3\text{H}$ ]STX. Employing concentrations ranging from 1 to 100  $\mu\text{M}$ , comparable to those that inhibited batrachotoxin-activated  $^{22}\text{Na}^+$  uptake, none of the antidepressants studied significantly altered [ $^3\text{H}$ ]STX binding (Fig. 1D). These results clearly indicate that the antidepressant block of voltage-gated  $\text{Na}^+$  channels cannot be attributed to an interaction at neurotoxin receptor site-1 of the  $\text{Na}^+$  channel.

Previous studies have shown that local anesthetics (Postma and Catterall, 1984) and anticonvulsants (Willow and Catterall, 1982) appear to reduce  $I_{\text{Na}}$  by inhibiting [ $^3\text{H}$ ]BTX binding via a negative allosteric interaction. In these studies, the site-3 neurotoxin, scorpion  $\alpha$ -toxin V ( $\alpha$ -LqqV) isolated from the venom of the scorpion *Leiurus q. quinquestriatus*, was used to increase the specific binding of [ $^3\text{H}$ ]BTX (Catterall, 1980). In the present study, both imipramine and amitriptyline produced a concentration-dependent inhibition of [ $^3\text{H}$ ]BTX binding in the presence of 0.3  $\mu\text{M}$   $\alpha$ -LqqV. Dose–response data were fitted by sigmoidal curves using the Logistic equation (Eq. (1) in Materials and methods) with  $K_i$  values of  $3.2 \pm 0.3$  and  $4.0 \pm 0.4 \mu\text{M}$  ( $n=4$ ), respectively, and a slope parameter ( $n_{\text{H}}$ ) of 1 indicating that there is no cooperativity between binding sites on synaptosomal  $\text{Na}^+$  channels (Fig. 1E). These results suggest that the inhibitory effect of antidepressants on the  $\text{Na}^+$  channel is mediated through an interaction with neurotoxin receptor site-2, reduction in the binding of  $\alpha$ -LqqV to site-3 or that a distinct imipramine binding site exists that regulates the affinity of batrachotoxin in a negative allosteric fashion.

#### 3.3. Effects of imipramine on $I_{\text{Na}}$

Rat dorsal root ganglion neurons express two main functional types of voltage-gated  $\text{Na}^+$  channels. Firstly, tetrodotoxin-sensitive  $\text{Na}^+$  channels, which are readily blocked by tetrodotoxin ( $K_i=0.3 \text{ nM}$ ) (Roy and Narahashi, 1992). Following the nomenclature system for voltage-gated  $\text{Na}^+$  channels (Goldin et al., 2000), these include  $\text{Na}_v1.1$ ,  $\text{Na}_v1.6$  and  $\text{Na}_v1.7$  subtypes that have been shown to be highly expressed in dorsal root ganglion neurons, together with  $\text{Na}_v1.2$ , which is expressed at low levels (Felts et al., 1997; Goldin, 2001). Secondly, tetrodotoxin-resistant (tetrodotoxin-resistant)  $\text{Na}^+$  channels, which are largely resistant to the action of tetrodotoxin ( $K_i=100 \mu\text{M}$ ) (Roy and Narahashi, 1992). These include the  $\text{Na}_v1.8$  and  $\text{Na}_v1.9$  channel subtypes (Goldin, 2001).

Imipramine exerted a concentration-dependent tonic block of both tetrodotoxin-sensitive and tetrodotoxin-resistant  $I_{\text{Na}}$ . Washing with drug-free solution restored peak tetrodotoxin-sensitive and tetrodotoxin-resistant  $I_{\text{Na}}$  within 15–20 min. Fig. 2A–C and E–G shows the effects of 3, 5 and 10  $\mu\text{M}$  imipramine on peak  $I_{\text{Na}}$  amplitude elicited by a

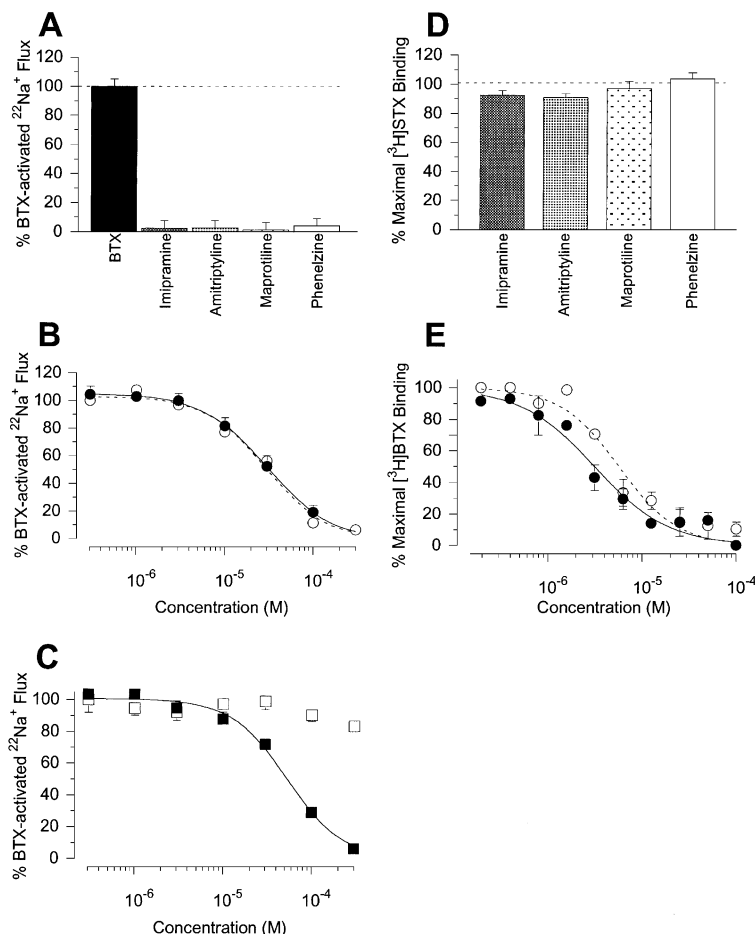


Fig. 1. Actions of antidepressants on  $^{22}\text{Na}^+$  uptake and radiolabelled neurotoxin receptor binding in rat brain synaptosomes. (A) Inability of antidepressants to directly activate  $^{22}\text{Na}^+$  uptake. Synaptosomes ( $500\ \mu\text{g}$ ) were incubated with antidepressants ( $100\ \mu\text{M}$ ) for 30 min at  $37\ ^\circ\text{C}$  and  $^{22}\text{Na}^+$  uptake measured after a 5-s period. Non-specific  $^{22}\text{Na}^+$  uptake in the presence of  $1\ \mu\text{M}$  tetrodotoxin was subtracted and data presented as a percentage of maximal uptake as determined in the presence of  $1\ \mu\text{M}$  batrachotoxin ( $n=3$ ). (B–C) Effects of antidepressants on batrachotoxin-stimulated  $^{22}\text{Na}^+$  uptake. Rat brain synaptosomes ( $500\ \mu\text{g}$ ) were incubated for 30 min at  $37\ ^\circ\text{C}$  with  $1\ \mu\text{M}$  batrachotoxin and increasing concentrations of antidepressants.  $^{22}\text{Na}^+$  uptake was then measured after 5 s. (B) Imipramine (—●—) and amitriptyline (—○—); (C) maprotiline (—■—) and phenezine (□). Non-specific  $^{22}\text{Na}^+$  uptake in the presence of  $1\ \mu\text{M}$  tetrodotoxin was subtracted and data presented as a percentage of maximal  $^{22}\text{Na}^+$  uptake as determined in the presence of  $1\ \mu\text{M}$  batrachotoxin ( $n=3-5$ ). (D) No alteration in  $[^3\text{H}]$ STX binding by antidepressants. Antidepressants ( $100\ \mu\text{M}$ ) were incubated with synaptosomes ( $300\ \mu\text{g}$ ) in the presence of  $2\ \text{nM}$   $[^3\text{H}]$ STX at  $37\ ^\circ\text{C}$  for 30 min. Data are presented as the percentage of maximal  $[^3\text{H}]$ STX binding following correction for non-specific binding determined in the presence of  $1\ \mu\text{M}$  tetrodotoxin. The dashed line represents maximal  $[^3\text{H}]$ STX binding. The data points represent the mean  $\pm$  S.E. of five experiments. (E) Inhibition of  $[^3\text{H}]$ BTX binding by antidepressants. Rat brain synaptosomes ( $350\ \mu\text{g}$ ) were preincubated with  $10\ \text{nM}$   $[^3\text{H}]$ BTX for 30 min at  $37\ ^\circ\text{C}$  in the presence of increasing concentrations of imipramine (—●—) or amitriptyline (—○—). The data points represent the mean  $\pm$  S.E. of four experiments. All concentration–response curves were fitted with Eq. (1). See Materials and methods for details of all experimental procedures.

50-ms depolarizing test pulse to  $-10\ \text{mV}$  from a holding potential of  $-80\ \text{mV}$  every 15 s. These concentration-dependent effects occurred over a narrow range of drug concentrations. Addition of  $30\ \mu\text{M}$  imipramine to the perfusion bath resulted in complete elimination of both types of  $I_{\text{Na}}$ , whilst  $100\ \text{nM}$  imipramine showed no indication of channel block.

The concentration–response curves for imipramine block of tetrodotoxin-sensitive and tetrodotoxin-resistant  $I_{\text{Na}}$  are shown in Fig. 2. The peak  $I_{\text{Na}}$  in the presence of imipramine was expressed as a percentage of the control peak  $I_{\text{Na}}$  and the depression of peak amplitude, after 10 min of perfusion, plotted against imipramine concentration. The data points are fitted by sigmoidal curves using the Logistic equation (Eq.

(1) in Materials and methods) based on  $n_{\text{H}}$  values of 1, 2 and 3. Clearly, the data best fit the curves calculated on the basis of  $n_{\text{H}}=2$ . Therefore, the cooperation of two molecules may be required in the blocking action of imipramine on both tetrodotoxin-sensitive and tetrodotoxin-resistant  $\text{Na}^+$  channels in dorsal root ganglion neurons. The larger  $n_{\text{H}}$  values for block of dorsal root ganglion neurons in comparison with polarized brain synaptosomes may reflect differences in the subtypes of  $\text{Na}^+$  channels in these tissues. However, it is also likely that since the inactivated state has a higher affinity for imipramine (see below) any binding will have a positive effect on subsequent binding yielding steeper dose–response curves with larger  $n_{\text{H}}$  values. The  $K_{\text{d}}$  values for inhibition of  $I_{\text{Na}}$  were determined to be  $5.2 \pm 0.2\ \mu\text{M}$  for tetrodotoxin-

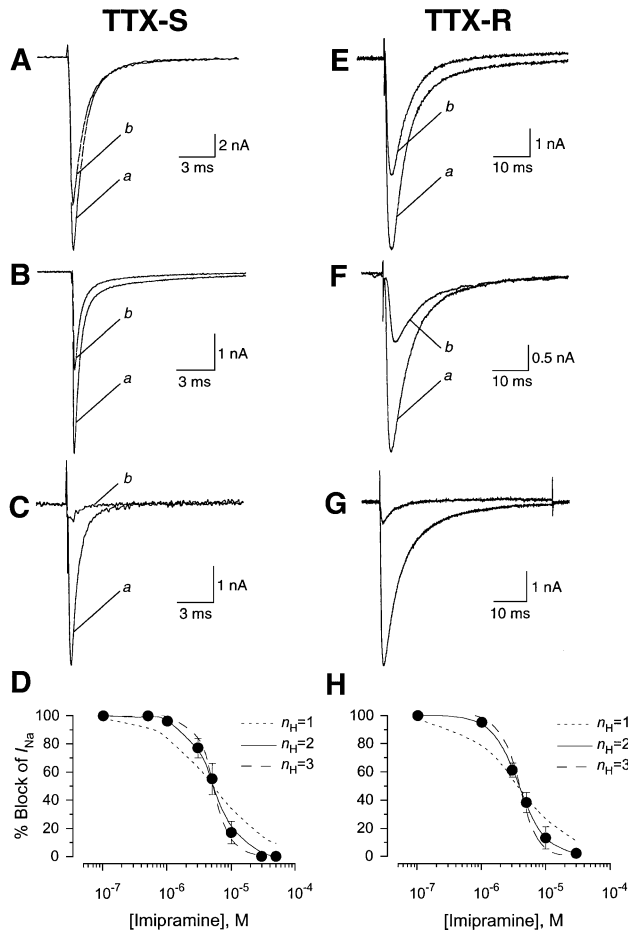


Fig. 2. Typical experiments showing concentration-dependent effects of imipramine on  $I_{Na}$  in rat dorsal root ganglion neurons. Effects of: 3  $\mu$ M (A,E), 5  $\mu$ M (B,F) and 10  $\mu$ M (C,G) imipramine on tetrodotoxin-sensitive (A–D) and tetrodotoxin-resistant (E–H)  $I_{Na}$  evoked by a 50-ms depolarization from a holding potential of  $-80$  mV (see inset) before (a) and 10 min after (b) the addition of imipramine. Tetrodotoxin-resistant  $I_{Na}$  was recorded in the presence of 200 nM tetrodotoxin to eliminate any residual tetrodotoxin-sensitive  $I_{Na}$ . (D,H) Concentration–response curves for inhibition of tetrodotoxin-A  $I_{Na}$  (D) and tetrodotoxin-resistant  $I_{Na}$  (H). Data were fitted with Eq. (1) in Materials and methods and represent the mean  $\pm$  S.E. of five experiments at each concentration.

sensitive  $I_{Na}$  ( $n=5$ ) and  $3.8 \pm 0.1$   $\mu$ M for tetrodotoxin-resistant  $I_{Na}$  ( $n=5$ ). Despite a profound blocking action on both tetrodotoxin-sensitive and tetrodotoxin-resistant  $I_{Na}$  currents, imipramine failed to alter the activation or inactivation kinetics, such that the time to peak current and the timecourse of current decay were not affected at concentrations of imipramine up to 10  $\mu$ M.

### 3.4. Effects on the voltage dependence of $Na^+$ channel activation

To determine whether tonic block reflected altered activation or permeability properties of  $Na^+$  channels we determined the action of imipramine on current–voltage relationships. A typical experiment shown in Fig. 3 details the current–voltage relationships before and after applica-

tion of 5  $\mu$ M imipramine for tetrodotoxin-sensitive and 3  $\mu$ M for tetrodotoxin-resistant  $I_{Na}$ . As shown in Fig. 3, imipramine had no effect on these parameters other than a reduction in peak  $I_{Na}$  amplitude. There was also little change observed in the reversal potential in post-drug recordings, indicating that the ionic selectivity of  $Na^+$  channels was not altered by imipramine.

To better quantify any drug-induced shifts in the voltage dependence of activation,  $g_{Na}$  values were determined according to Eq. (3) of Materials and methods. Conductance data were then normalized and averaged across all experiments. Similar thresholds of activation in pre- and post-drug conditions were observed for both tetrodotoxin-sensitive and tetrodotoxin-resistant  $g_{Na}$ . Fitting of the data to Boltzmann distributions (Eq. (4) in Materials and methods) revealed that there was no shift in the voltage midpoint of activation of tetrodotoxin-sensitive  $g_{Na}$  (control  $V_{1/2} = -24.4 \pm 1.1$  vs. drug  $V_{1/2} = -24.5 \pm 0.7$  mV,  $n=5$ ) nor was there a signifi-

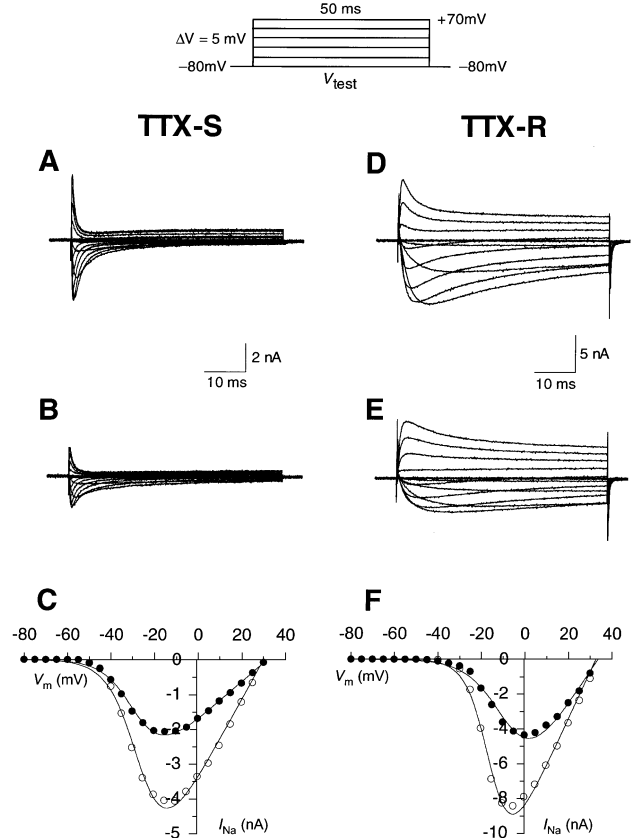


Fig. 3. Effects of imipramine on the current–voltage relationship. Currents were evoked by a series of 50-ms depolarizations from a holding potential of  $-80$  mV. Test voltages ranged from  $-80$  to  $+70$  mV in 10-mV steps and were delivered every 10 s (see inset). Families of tetrodotoxin-sensitive (left-hand panels) and tetrodotoxin-resistant (right-hand panels)  $I_{Na}$  recorded before (A,D) and after 5  $\mu$ M (B) and 3  $\mu$ M (E) imipramine at 16  $^{\circ}$ C. For clarity, only  $I_{Na}$  recorded in 20-mV steps is presented. (E–F) Peak current/voltage ( $I/V$ ) relationships are graphed for the same experiment shown in (A)–(D) in the absence (○) and presence (●) of 5  $\mu$ M (C) and 3  $\mu$ M (F) imipramine. Data were fitted with Eq. (2) in Materials and methods.

cant change in the slope factor (control  $s = 10.6 \pm 0.7$  vs. drug  $s = 11.2 \pm 0.6$ ). Tetrodotoxin-resistant  $g_{\text{Na}}$  demonstrated a slight depolarizing shift in activation from  $-6.4 \pm 0.6$  in controls to  $-1.43 \pm 0.57$  mV in imipramine ( $n = 4$ ) without a change in the slope factor (control  $s = 12.7 \pm 0.6$  vs. drug  $s = 13.5 \pm 0.4$ ,  $n = 4$ ). However, the small magnitude of the shift (less than 5 mV) would be unlikely to have any physiological ramifications.

### 3.5. Effects of imipramine on the voltage dependence of steady-state $\text{Na}^+$ channel inactivation ( $h_{\infty}$ )

Measurements were made using a standard two-pulse protocol as shown at the top of Fig. 4. The amplitude of the peak current associated with the test pulse was plotted as a function of the conditioning prepulse potential. In the presence of imipramine (3–5  $\mu\text{M}$ ) the maximum  $I_{\text{Na}}$  decreased by approximately 50% at large negative prepulse potentials ( $-120$  to  $-130$  mV for tetrodotoxin-sensitive  $I_{\text{Na}}$  and  $-80$  to  $-130$  mV for tetrodotoxin-resistant  $I_{\text{Na}}$ ). This is comparable to that seen in the concentration–response curves in Fig. 2. When the maximum current in the presence of imipramine was normalized to that of the control, a parallel shift in the hyperpolarizing direction was observed (Fig. 4C,D). Imipramine caused a significant hyperpolarizing shift in the voltage at which half of the tetrodotoxin-sensitive  $I_{\text{Na}}$  were inactivated ( $V_{1/2}$ ), from  $-66 \pm 2$  in controls to  $-80 \pm 2$  mV in the presence of imipramine ( $\Delta V_{1/2} = -18$  mV,  $P < 0.008$ ,  $n = 5$ ). Similarly,  $V_{1/2}$  values for tetrodotoxin-resistant  $I_{\text{Na}}$  were shifted from  $-40 \pm 2$  in controls to  $-46 \pm 2$  mV in the presence of imipramine ( $\Delta V_{1/2} = -6$  mV,  $P < 0.05$ ,  $n = 6$ ). The slope ( $k$ ) of the steady-state inactivation curve was unaffected by imipramine in both instances. Thus, block of voltage-gated  $\text{Na}^+$  channels by imipramine is voltage-dependent as evidenced by a shift in the voltage-dependence of steady-state inactivation. The shift in  $h_{\infty}$  could result from a higher affinity of imipramine for the inactivated rather than the resting state of the channel. For example at negative holding potentials ( $-130$  mV) all tetrodotoxin-sensitive  $\text{Na}^+$  channels exist in the resting state and thus the block by imipramine represents resting block with an apparent dissociation constant of 5  $\mu\text{M}$ . At less negative holding potentials ( $-80$  mV), at which 30% of the total channels are in the inactivated state (Fig. 4B), the block by imipramine is markedly enhanced. Therefore, under conditions where the membrane is more depolarized the block by imipramine is more pronounced due to this state-dependent binding. These results indicate that imipramine has a higher affinity for the inactivated state of the channel.

### 3.6. Use-dependent block of $I_{\text{Na}}$ by imipramine

The actions of local anesthetics, antiarrhythmics, anti-convulsants and neuroleptics such as chlorpromazine are known to be modified by high-frequency stimulation (Ogata

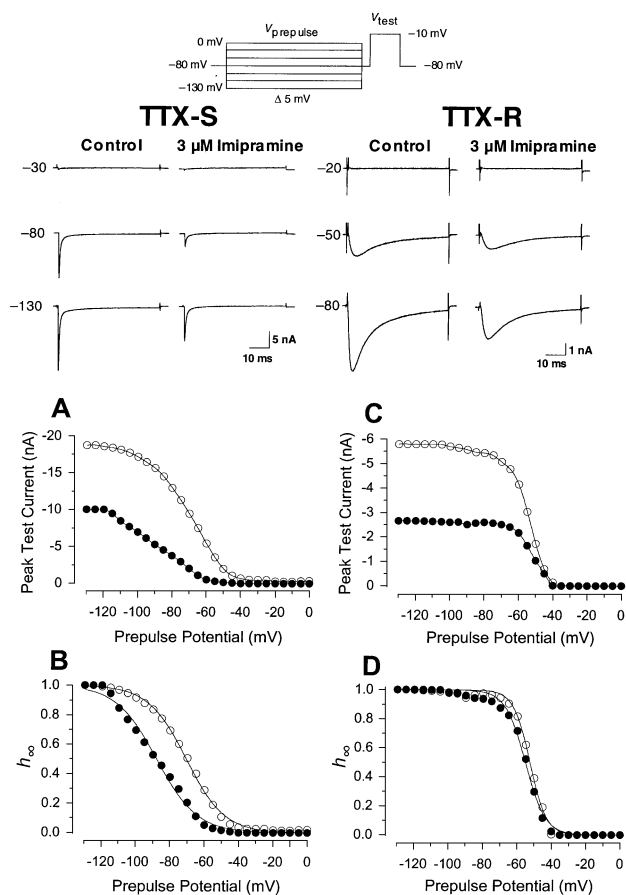


Fig. 4. Typical effects of imipramine on steady-state  $\text{Na}^+$  channel inactivation ( $h_{\infty}$ ). Steady-state channel inactivation was determined using a two-pulse protocol (see inset). Conditioning prepulses of 1000 ms duration ranging from  $-130$  to  $0$  mV were delivered in  $5$ -mV steps. Typical current traces obtained following a  $50$ -ms test pulse to  $-10$  mV subsequent to prepulse potentials of  $-130$ ,  $-80$  and  $-30$  mV before (left-hand trace) and following a  $10$ -min perfusion with imipramine (right-hand traces). Peak  $I_{\text{Na}}$  was recorded during the test pulse and normalized to the maximum peak  $I_{\text{Na}}$  and plotted against prepulse potential. The amount of  $I_{\text{Na}}$  that is available for activation during the test pulse under control conditions ( $\circ$ ) and during imipramine ( $\bullet$ ) is shown. (A) shows the effect of  $5$   $\mu\text{M}$  imipramine on tetrodotoxin-sensitive  $I_{\text{Na}}$  whilst (C) shows the effect of  $3$   $\mu\text{M}$  imipramine on tetrodotoxin-resistant  $I_{\text{Na}}$ . The amount of  $I_{\text{Na}}$  available for activation at any given membrane potential for control conditions ( $\circ$ ) and  $10$  min after perfusion of imipramine ( $\bullet$ ) is shown. (B,D) Currents were normalized to the maximum control current. Curves in (C) and (D) were fitted according to Eq. (5) described in Materials and methods.

and Narahashi, 1989; Ogata and Tatebayashi, 1989; Ragsdale et al., 1991, 1996). Consequently, the effects of imipramine peak  $I_{\text{Na}}$  were examined during rapid trains of pulses delivered at 1, 3, 10 and 30 Hz delivered 90 s apart to allow for recovery from use-dependent block. Fig. 5 shows a typical experiment where currents were evoked by 10 consecutive pulses to  $-10$  mV, for 30 ms, applied from a holding potential of  $-80$  mV. In the control recordings there was a steady decline in current amplitude which increased at higher stimulation frequencies. In the presence of imipramine there was an additional decline in the currents. Fig. 5

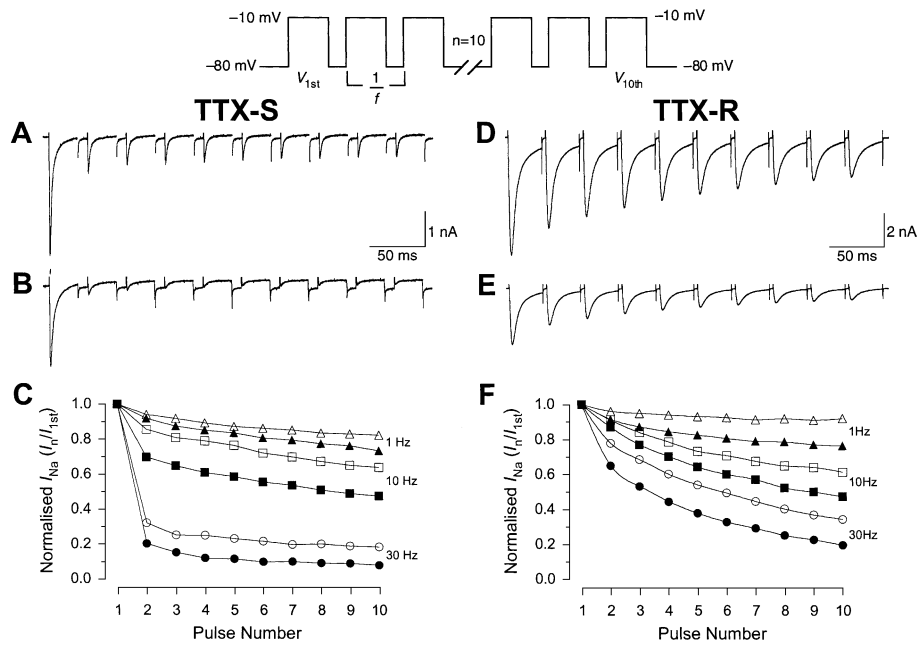


Fig. 5. Use-dependent actions of imipramine during pulse trains. A typical experiment showing the effects of imipramine on use-dependent decline in tetrodotoxin-sensitive (left-hand panels) and tetrodotoxin-resistant (right-hand panels)  $I_{Na}$  during 10 depolarizing test pulses from  $-80$  to  $-10$  mV at 1 ( $\Delta$ ,  $\blacktriangle$ ), 10 ( $\square$ ,  $\blacksquare$ ), and 30 Hz ( $\circ$ ,  $\bullet$ ). Panels (A)–(D) show typical current traces recorded during depolarizing test pulses applied at a frequency of 30 Hz obtained before (A,D) and 10 min after perfusion with 5  $\mu$ M (B) and 3  $\mu$ M imipramine (E). (C,F) Currents were normalized to the peak current amplitude of the first pulse in the train ( $I_{1st}$ ) in the absence (open symbols) and presence of imipramine (filled symbols).

shows the time course of  $I_{Na}$  elicited at each frequency. The peak  $I_{Na}$  at each test pulse ( $I_n$ ) was normalized to that of the peak  $I_{Na}$  during the first test pulse ( $I_{1st}$ ) and plotted as a function of the pulse number. A marked cumulative decrease in peak  $I_{Na}$  was seen at each consecutive pulse. In the presence of imipramine, however, this decline was accentuated due to the accumulation of use-dependent block. Increasing the frequency of stimulation resulted in an increase in the extent of use-dependent block. These results were typical of five experiments on tetrodotoxin-sensitive  $I_{Na}$  and six experiments on tetrodotoxin-resistant  $I_{Na}$ .

### 3.7. Effects on the rate of $Na^+$ channel recovery from inactivation

The above actions on steady-state  $Na^+$  channel inactivation and the development of a use-dependent block indicate that imipramine binds to, and stabilizes, the inactivated state of  $Na^+$  channels. As a result, the repriming kinetics of the  $Na^+$  channel is expected to be delayed by imipramine. To investigate this possibility, a standard two-pulse protocol with a variable interpulse interval was employed. A conditioning prepulse for 100 or 300 ms (tetrodotoxin-sensitive and tetrodotoxin-resistant  $I_{Na}$ , respectively) to  $-10$  mV was used to completely inactivate channels, and after the designated interpulse interval, ranging between 0.5 ms and 1 s, peak  $I_{Na}$  was recorded during a 50-ms depolarizing test pulse to the same potential. The two-pulse protocols were delivered 45 s apart. Peak  $I_{Na}$  during the test pulse ( $I_{test}$ ) was normalized to that of the

preceding conditioning pulse ( $I_{cond}$ ) and plotted as a function of interpulse interval ( $\Delta T$ ).

Under control conditions, the rate of recovery of tetrodotoxin-sensitive and tetrodotoxin-resistant  $I_{Na}$  was fitted by double exponential functions (Eq. (6) in Materials and methods). Recovery was essentially complete within 2 s for tetrodotoxin-sensitive  $I_{Na}$  and 2.6 s for tetrodotoxin-resistant  $I_{Na}$ . In the presence of imipramine, the rate of recovery was fitted by a double exponential function; however, the time course of recovery was slowed for both tetrodotoxin-sensitive and tetrodotoxin-resistant  $I_{Na}$ . Fig. 6 shows a typical experiment. The lower panels in Fig. 6 show the semilogarithmic transformation of the unrecovered fraction of peak current used to quantify the rate of recovery from inactivation. Both the fast time constant of recovery ( $\tau_f$ ) and the slow time constant of recovery ( $\tau_s$ ) were slowed by imipramine; however, the fractions of recovery of  $\tau_f$  and  $\tau_s$  were not significantly altered. These results are representative of those obtained in seven experiments on tetrodotoxin-sensitive  $I_{Na}$  and nine experiments on tetrodotoxin-resistant  $I_{Na}$  (see Table 1).

### 3.8. $K^+$ currents in rat dorsal root ganglion neurons

Dorsal root ganglia voltage-gated  $K^+$  channel currents can be divided into at least three main functional subtypes: the delayed-rectifier ( $I_{K(DR)}$ ), transient 'A-type' ( $I_T$ ), and inward-rectifier ( $I_{K(IR)}$ ) (Ogata and Tatebayashi, 1993; Safro-nov et al., 1996; Fedulova et al., 1998). These can be differentiated by a combination of gating kinetic properties

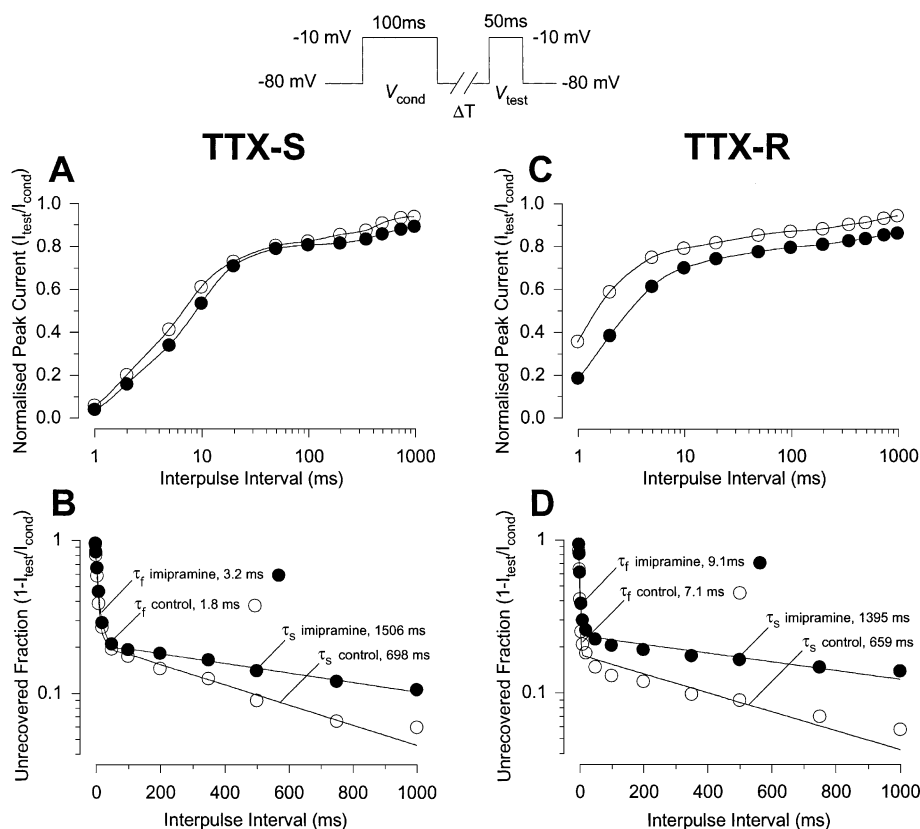


Fig. 6. Effects of imipramine on  $\text{Na}^+$  channel repriming kinetics. The rate of channel repriming was assessed using a standard two-pulse protocol as illustrated in the inset where  $\Delta T$  represents the interpulse intervals. Sodium channel repriming rate was determined by normalizing peak  $I_{\text{Na}}$  elicited during  $V_{\text{test}}$  against peak currents recorded during  $V_{\text{cond}}$  and plotted as a function of the interpulse interval. Left-hand panels show the effects of  $5 \mu\text{M}$  imipramine on tetrodotoxin-sensitive  $I_{\text{Na}}$  while the right-hand panels show the effects of  $3 \mu\text{M}$  imipramine on tetrodotoxin-resistant  $I_{\text{Na}}$ . Representative graphs recorded before (○) and 10 min after perfusion with imipramine (●) with interpulse intervals ranging from 0.5 to 1000 ms. Panels (A) and (C) show the recovery from inactivation plotted as a function of the interpulse intervals. Panels (B) and (D) show the magnitude of the unrecovered fraction of the data from (A) and (B) plotted on a semi-logarithmic scale. Data in panels (B) and (D) were fitted as the sum of two exponential functions according to Eq. (6) described in Materials and methods.

and pharmacological blocking agents (see Materials and methods). We have examined the actions of imipramine on these three voltage-gated  $\text{K}^+$  channel functional subtypes.

### 3.9. Effects of imipramine on $I_{\text{K}}$

Imipramine exerted a concentration-dependent depression of peak  $I_{\text{K(DR)}}$  amplitude. Fig. 7 shows the typical effects of 1, 10, 30 and 1000  $\mu\text{M}$  imipramine on peak  $I_{\text{K(DR)}}$

amplitude elicited by a standard 250-ms depolarizing pulse from  $-40$  to  $-10$  mV. The concentration–response data were fitted by sigmoidal curves using the Logistic equation (Eq. (1) in Materials and methods) based on  $n_{\text{H}}$  values of 1 and 2. Clearly, the data best fit the curves calculated on the basis of  $n_{\text{H}} = 1$ . The dissociation constant ( $K_{\text{d}}$ ) was found to be  $46 \pm 3 \mu\text{M}$  ( $n = 4-7$ ).

We found that  $I_{\text{T}}$  was preferentially expressed in larger neurons and confined our study of  $I_{\text{T}}$  to cells having

Table 1  
Effects of imipramine on the rate of recovery from  $\text{Na}^+$  channel inactivation

Parameter <sup>a</sup>	Tetrodotoxin-sensitive $I_{\text{Na}}$			Tetrodotoxin-resistant $I_{\text{Na}}$		
	Control	5 $\mu\text{M}$ Imipramine	<i>P</i>	Control	3 $\mu\text{M}$ Imipramine	<i>P</i>
$\tau_{\text{f}}$ (ms)	$6.8 \pm 1.1$	$8.9 \pm 1.4$	$<0.045$	$2.8 \pm 0.2$	$4.4 \pm 0.5$	$<0.04$
<i>A</i>	$0.79 \pm 0.04$	$0.83 \pm 0.03$	NS <sup>b</sup>	$0.74 \pm 0.03$	$0.74 \pm 0.03$	NS
$\tau_{\text{s}}$ (ms)	$673 \pm 124$	$1459 \pm 197$	$<0.003$	$810 \pm 93$	$1498 \pm 196$	$<0.003$
<i>B</i>	$0.21 \pm 0.04$	$0.17 \pm 0.03$	NS	$0.26 \pm 0.03$	$0.26 \pm 0.03$	NS

The time constants  $\tau_{\text{f}}$  and  $\tau_{\text{s}}$  represent fast and slow recovery from inactivation, respectively, in ms. *A* and *B* represent fractions of recovery described by  $\tau_{\text{f}}$  and  $\tau_{\text{s}}$ , respectively.

<sup>a</sup> Parameters were calculated by fitting to a double exponential decay function (see Eq. (6) in Materials and methods). Data are presented as the mean  $\pm$  S.E. for tetrodotoxin-sensitive ( $n = 7$ ) and tetrodotoxin-resistant ( $n = 9$ )  $I_{\text{Na}}$ .

<sup>b</sup> Not significant at  $P < 0.05$ .

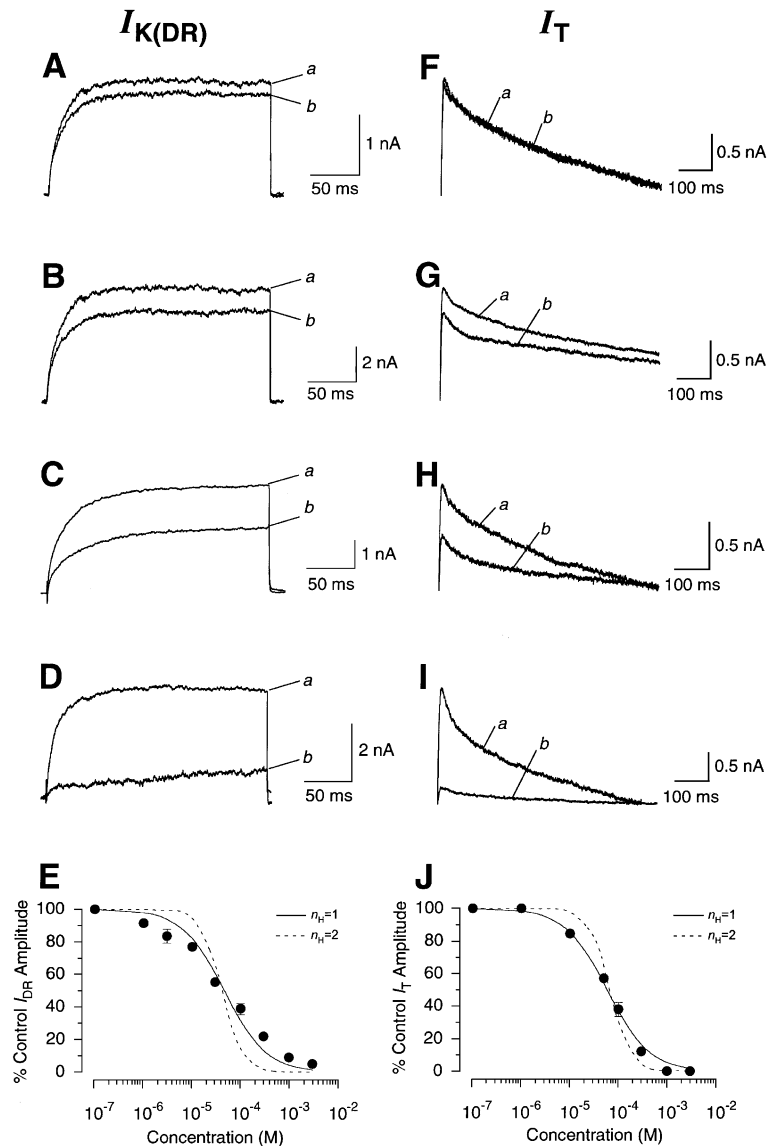


Fig. 7. Concentration-dependent effects of imipramine on  $K^+$  currents in dorsal root ganglion neurons. (A–D) Representative effects of 1  $\mu\text{M}$  (A), 10  $\mu\text{M}$  (B), 30  $\mu\text{M}$  (C) and 1 mM (D) imipramine on  $I_{K(DR)}$  elicited by a 250-ms depolarizing test pulse to  $-10$  mV from a holding potential of  $-40$  mV before (a) and 10 min after (b) the addition of imipramine (b). All currents were recorded in the presence of 1 mM 4-aminopyridine. (F–I) Effects of 1  $\mu\text{M}$  (F), 50  $\mu\text{M}$  (G), 100  $\mu\text{M}$  (H) and 300  $\mu\text{M}$  (I) imipramine on the transient ('A'-type) current ( $I_T$ ) before (a) and 10 min after (b) the addition of imipramine.  $I_T$  was elicited by a two-pulse protocol, from a holding potential of  $-40$  mV and consisted of a 2300-ms hyperpolarizing pulse to  $-120$  mV followed by a 700-ms test pulse to  $-40$  mV. At this potential,  $I_{DR}$  was not activated and thus  $I_T$  could be evoked in isolation. In addition, 25 mM tetraethylammonium-Cl was added to block any residual  $I_{DR}$ . (E, J) Concentration–response curves for inhibition of  $I_{K(DR)}$  (E) and  $I_T$  (J). Data were fitted with Eq. (1) in Materials and methods and represent the mean  $\pm$  S.E. of 4–7 experiments at each concentration.

diameters larger than 35  $\mu\text{m}$ . Similar to its effects on  $I_{K(DR)}$ , imipramine also exerted a concentration-dependent depression of peak  $I_T$ . Fig. 7 shows the typical effects of 1, 50, 100 and 300  $\mu\text{M}$  imipramine on peak  $I_T$  amplitude elicited using a pulse protocol that hyperpolarizes the membrane potential to  $-120$  mV from a holding potential of  $-40$  mV for 2300 ms followed by a step back to  $-40$  mV. The concentration–response data was fitted by the Logistic equation and the dissociation constant ( $K_d$ ) was found to be  $61 \pm 4$   $\mu\text{M}$  best fitted with a Hill coefficient ( $n_H$ ) of 1 ( $n=4-7$ ). No effects were observed with 100  $\mu\text{M}$  imipramine on  $I_{K(IR)}$ , however,

approximately 50% block was evident at 1000  $\mu\text{M}$  (data not shown).

### 3.10. Effects on the voltage dependence of $K^+$ channel activation

Current–voltage relationships for  $I_{K(DR)}$  were examined using 250-ms test pulses to various membrane potentials ranging between  $-50$  and  $+50$  mV in 10-mV steps, from a holding potential of  $-40$  mV. To prevent contamination by  $I_T$ , 1 mM 4-aminopyridine was added to the external bathing

solution. A typical experiment showing the current–voltage relationship for  $I_{K(DR)}$  before and after application of 30  $\mu\text{M}$  imipramine is shown in Fig. 8. Under control conditions an outward  $I_{K(DR)}$  was activated in response to a depolarizing test pulse at potentials greater than +40 mV, inward rectification was not evident even at potentials of +50 mV (Fig. 8A). Following perfusion with 30  $\mu\text{M}$  imipramine there was no alteration in the time course or voltage-dependence of channel activation. The only observed change was the reduction in peak amplitude at all membrane potentials (Fig. 8C). The results presented here were confirmed in nine other experiments. To quantify any drug-induced shifts in the voltage dependence of activation,  $g_{K(DR)}$  values were determined according to Eq. (3) of Materials and methods. Conductance data were then normalized and averaged across all experiments. Fitting of the data to Boltzmann distributions (Eq. (4) in Materials and methods) revealed that there was no shift in the voltage midpoint of activation of  $g_{K(DR)}$  (control  $V_{1/2} = 22.1 \pm 1.1$  vs. drug  $V_{1/2} = 24.7 \pm 2.6$  mV,  $n = 9$ ) nor was there a significant change in the slope factor (control  $s = 16.9 \pm 1.5$  vs. drug  $s = 16.5 \pm 1.6$ ).

Current–voltage relationships for the  $I_T$  were examined using a two-pulse protocol, shown above Fig. 8B. As before 25 mM of tetraethylammonium-Cl was added to block any residual  $I_{K(DR)}$ . The blocking effect of 100  $\mu\text{M}$  imipramine was resistant to washout with drug-free solution with only a partial reversal following washout for 10 to 20 min. A typical

experiment showing the current–voltage relationship for  $I_T$  before and after applications of 100  $\mu\text{M}$  imipramine is shown in Fig. 8D–F. Under control conditions the outward  $I_T$  was activated in response to a depolarizing test pulse at potentials greater than –60 mV. Following perfusion with imipramine there was no alteration to the voltage-dependence of channel activation or changes in the rate of inactivation. The only observed change was the reduction in peak  $I_T$  amplitude. The results presented here were confirmed in eight other experiments. Fitting of the data to Boltzmann distributions (Eq. (4) in Materials and methods) revealed that there was no shift in the voltage midpoint of activation (control  $V_{1/2} = -30.4 \pm 2.5$  vs. drug  $V_{1/2} = -33.6 \pm 2.6$  mV,  $n = 5$ ) nor was there a significant change in the slope factor (control  $s = 14.3 \pm 2.2$  vs. drug  $s = 12.7 \pm 1.7$ ).

Current–voltage relationships for the  $I_{K(IR)}$  were examined using 700-ms hyperpolarizing test pulses to various membrane potentials ranging between –80 and –130 mV from a holding potential of –70 mV in 10-mV steps. A typical experiment showing the current–voltage relationship for  $I_{K(IR)}$  before and after application of 100  $\mu\text{M}$  imipramine is shown in Fig. 8G–I. Under control conditions the outward  $I_{K(IR)}$  was activated in response to a hyperpolarizing test pulse at potentials less than –80 mV. Following perfusion with 100  $\mu\text{M}$  imipramine there was no alteration to the threshold of channel activation or kinetics.

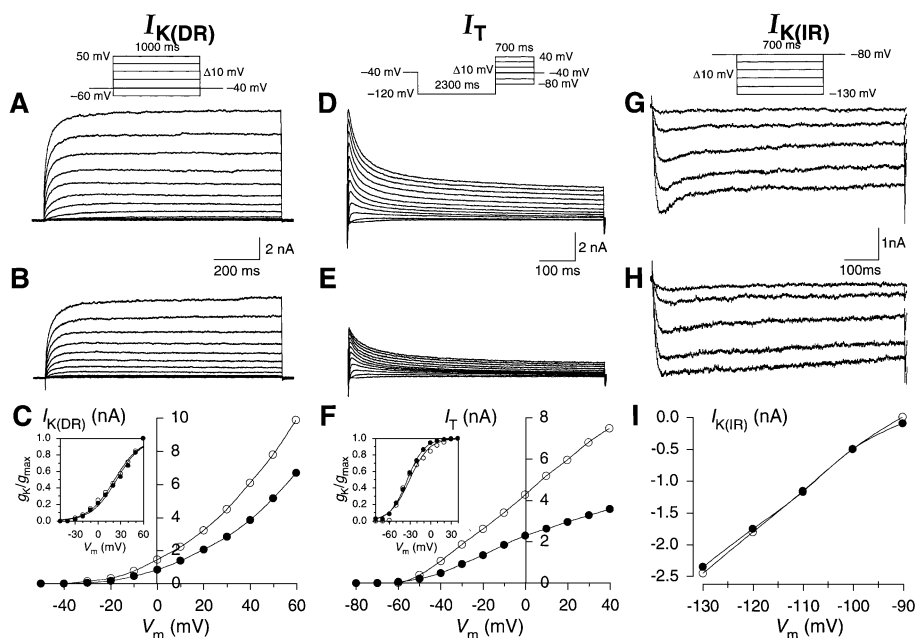


Fig. 8. Typical effects of imipramine on the current–voltage relationships for  $K^+$  currents in dorsal root ganglion neurons. (A–C) Typical  $I_{K(DR)}$  currents elicited by a 250-ms test pulses from –50 to 60 mV in 10-mV steps in the presence of 1 mM 4-aminopyridine, using the pulse protocol shown above (A). (D–F) Typical  $I_T$  currents elicited by 700-ms test pulses from –80 to 40 mV in 10-mV steps, using the pulse protocol indicated above (D). (G–I) Typical  $I_{K(IR)}$  currents elicited by 700-ms test pulses from –80 to –130 mV in 10-mV steps, using the pulse protocol shown above (G). Upper panels (A,D,G) show control currents. Middle panels (B,E,H) show the effect on  $K^+$  currents recorded following a 10-min perfusion with 30  $\mu\text{M}$  (B), 100  $\mu\text{M}$  (E) and 100  $\mu\text{M}$  (H) imipramine. Lower panels (C,F,I) show current–voltage relationships for  $I_{K(DR)}$ ,  $I_T$  and  $I_{K(IR)}$  peak currents plotted as a function of membrane potential in the absence (○) and presence of imipramine (●). Insets in (C) and (F) show normalized conductance curves ( $g_K/g_{max}$ ) for  $I_{K(DR)}$  and  $I_T$  currents. Note the lack of alteration in the voltage of dependence of activation following perfusion with imipramine.

#### 4. Discussion

The present results show that a structurally diverse group of antidepressant drugs bind with voltage-gated  $\text{Na}^+$  channels to inhibit  $I_{\text{Na}}$ . Whilst there is a tonic block of  $\text{Na}^+$  channels produced by imipramine there is also strong evidence to indicate a use-dependent block of these channels. It would therefore appear that the blocking action of imipramine can be interpreted on the basis of the modulated receptor hypothesis of [Hondeghem and Katzung \(1977\)](#) developed for local anesthetic block of  $\text{Na}^+$  channels which postulated preferential binding of the drugs to the inactivated state of the channel. Since imipramine has a higher affinity for the inactivated state of the  $\text{Na}^+$  channel a use-dependent block occurs because the proportion of the time spent in the inactivated state progressively increases during a repetitive train of depolarizing pulses. Therefore drug bound during one stimulus cannot completely dissociate by the next pulse. This type of use-dependent block has been described for other therapeutic agents including local anesthetics, phenytoin, carbamazepine and neuroleptics such as chlorpromazine ([Willow et al., 1985](#); [Ogata and Tatebayashi, 1989](#); [Ragsdale et al., 1991, 1996](#)).

Despite being unable to measure the  $K_d$  of imipramine for the activated state of the channel it must be higher than  $K_{\text{rest}}$  and  $K_{\text{inact}}$  for two reasons. Firstly, imipramine did not increase the decay kinetics of  $I_{\text{Na}}$  normally seen with open channel blockers where the drug binding rate is faster for the open channel than the inactivated channel ([Colquhoun and Hawkes, 1983](#)). Secondly, imipramine failed to alter the shape of the  $I/V$  relationship ([Fig. 3C,F](#)). If imipramine had a higher affinity for the open state of the channel then block of  $I_{\text{Na}}$  would have been more apparent when the majority of channels are open, i.e. more positive than  $-10$  mV in tetrodotoxin-sensitive  $\text{Na}^+$  channels and  $+10$  mV in tetrodotoxin-resistant  $\text{Na}^+$  channels.

The use-dependent effects shown here are remarkably similar to those exhibited by the anticonvulsants carbamazepine and phenytoin ([Willow et al., 1985](#)), which exert their therapeutic action by a use-dependent inhibition of  $\text{Na}^+$  channels due to preferential binding of drug to inactivated channels ([Willow et al., 1985](#)). The present study also shows that inactivated  $\text{Na}^+$  channels undergo a transition to the resting state after depolarization at a slower rate in the presence of imipramine, indicating a prolongation of the refractory period. A variety of other drugs such as the anticonvulsants phenytoin and carbamazepine ([Willow et al., 1985](#)), the antiarrhythmic verapamil ([Ragsdale et al., 1991](#)), and the local anesthetic tetracaine ([Ragsdale et al., 1991](#)) all slow the rate of  $\text{Na}^+$  channel recovery from inactivation. This slowed rate of recovery from inactivation reflects either slow drug dissociation from the inactivated or resting states or slow conversion of channels from the inactivated to the resting states consistent with the use-dependent block of  $\text{Na}^+$  channels.

In the present study, we observed that antidepressants failed to directly activate  $^{22}\text{Na}^+$  uptake but potently inhibited batrachotoxin-activated  $^{22}\text{Na}^+$  uptake in rat brain synaptosomes in a similar fashion to that observed in veratridine-induced  $^{22}\text{Na}^+$  flux in adrenal medullary cells ([Arita et al., 1987](#)). This inhibition of  $^{22}\text{Na}^+$  uptake did not occur via an interaction with site-1 since we found that a range of antidepressants did not inhibit [ $^3\text{H}$ ]STX binding. This is supported by the findings of [Arita et al. \(1987\)](#) who found that saxitoxin did not compete for inhibition of [ $^3\text{H}$ ]imipramine binding in adrenal medullary cells.

We report that tricyclic antidepressants produce a dose-dependent inhibition of batrachotoxin binding. The observed inhibition of [ $^3\text{H}$ ]BTX binding and the reduction in batrachotoxin-activated  $^{22}\text{Na}^+$  flux could therefore be due to a direct competitive displacement of batrachotoxin by the antidepressants or negative allosteric interactions at neurotoxin receptor site-2. Previous neurochemical experiments found that phenytoin, carbamazepine ([Willow and Catterall, 1982](#)), and tetracaine ([Postma and Catterall, 1984](#)) all interact with neurotoxin site-2, via a negative allosteric mechanism. The present patch clamp experiments indicate that imipramine preferentially binds to non-conducting states of the channel particularly the inactivated state and stabilizes these states. Since the  $^{22}\text{Na}^+$  uptake experiments were performed in synaptosomes where the resting membrane potential is slightly more positive than  $-60$  mV a significant percentage of the channels will be inactivated. Thus, the action of site-2 toxins such as batrachotoxin is to shift the inactivated channels into the open state. Imipramine indirectly competes with this process by stabilizing the inactivated state that has low affinity for site-2 toxins thus resulting in a negative allosteric inhibition of [ $^3\text{H}$ ]BTX binding. However, [Arita et al. \(1987\)](#) found that the site-2 partial agonist, veratridine, does not compete for [ $^3\text{H}$ ]imipramine binding. This apparent lack of interaction with site-2 may reflect differences in the action of antidepressants or site-2 toxins or differences in the subtypes of  $\text{Na}^+$  channels in adrenal medullary cells in comparison with brain synaptosomes.

In contrast to its non-selective actions on voltage-gated  $\text{Na}^+$  channels, imipramine was 1.3-fold more potent at blocking  $I_{\text{K(DR)}}$  than  $I_{\text{T}}$ , but was practically inactive on  $I_{\text{K(IR)}}$  ( $K_d > 1$  mM). Despite profound blocking effects of imipramine on outward  $\text{K}^+$  channel subtypes, imipramine did not alter the voltage-dependence of activation or the timecourse of inactivation. The selectivity of block is similar in cardiac myocytes and sympathetic neurons ([Delpón et al., 1991, 1992](#); [Wooltorton and Mathie, 1995](#)) although imipramine appears to be less potent on  $\text{K}^+$  channels in dorsal root ganglion neurons than other neuronal or cardiac cells ([Ogata et al., 1989b](#); [Delpón et al., 1992](#); [Wooltorton and Mathie, 1995](#)).

There is considerable difficulty in determining if these effects of antidepressants are clinically relevant given the wide variance in reported plasma concentrations. Never-

theless, it is commonly regarded that imipramine plasma concentrations of around 200 ng/ml (100–300 ng/ml) are considered to be therapeutic (see Benet and Williams, 1990). However, it would appear that tricyclic antidepressant drugs accumulate in brain tissue with a brain/plasma drug concentration ratio of between 8:1 and 40:1 (Glotzbach and Preiskorn, 1982). At therapeutic plasma concentrations, the brain concentration for imipramine ( $M_r$  280.4) can therefore be expected to be between 1.6 and 8  $\mu\text{g/ml}$ , equivalent to 5.4–27.2  $\mu\text{M}$  given a brain tissue specific gravity of 1.050 (Nelson et al., 1971). In overdose cases, toxicity can be expected above plasma concentrations of 1  $\mu\text{g/ml}$ . These studies therefore provide quantitative confirmation of the significance of effects on voltage-gated  $\text{Na}^+$  channels at supratherapeutic and even therapeutic antidepressant concentrations. Although the  $K_d$  values for block of  $I_{K(\text{DR})}$  and  $I_T$  were higher than for  $I_{\text{Na}}$ , it was also evident from the concentration–response curves that >30% block of these currents occurs at concentrations higher than 20  $\mu\text{M}$ . It is therefore reasonable to predict that significant inhibition of  $\text{Na}^+$  and  $\text{K}^+$  channels will occur which can profoundly alter cellular excitability.

Potassium channels are important regulators of neuronal membrane potential and neuronal excitability. Drugs that interact with neuronal  $\text{K}^+$  channels would therefore have profound effects on cellular signaling. It has already been shown that the tricyclic antidepressant desipramine can prolong the terminal action potential in rat sympathetic neurons resulting in increased transmitter release (Bennett and Middleton, 1975). The results presented here suggest that this can be explained by a blockade of  $I_{K(\text{DR})}$  and complement the findings of Wooltorton and Mathie (1995). Inhibition of  $I_T$  may also contribute to the underlying proconvulsant and proarrhythmic adverse-effects of imipramine. A direct mechanism of antidepressant epileptogenesis is postulated by the study by Ogata and Tatebayashi (1993) examining the effects of the neuroleptic chlorpromazine on dorsal root ganglion  $\text{K}^+$  channels. Their results indicate that chlorpromazine exerts a potent blocking action, which, given the importance of  $I_T$  for neuronal repolarization, suggests a mechanism by which chlorpromazine could induce seizures. Tricyclic antidepressants would be likely to exert similar effects. The  $I_T$  seen in dorsal root ganglion neurons also has similar properties to the slowly inactivating  $\text{K}^+$  currents found in nodose and hippocampal neurons which have previously been shown to play an important role in limiting firing frequency. Inhibition of this current can induce profound repetitive firing of action potentials (Stansfeld et al., 1986). Other agents that block  $I_T$  such as 4-aminopyridine have also been shown to induce repetitive firing in rat dorsal root fibres (Baker et al., 1985). Thus imipramine may affect cellular excitability through a blockade of  $I_T$ .

In conclusion, this study shows that imipramine produces differential inhibition of various subtypes of voltage-gated  $\text{Na}^+$  and  $\text{K}^+$  channels. At therapeutically relevant doses, the interaction of imipramine with  $\text{Na}^+$  channels may result in

adverse effects such as antiarrhythmic and sedative actions. Conversely, the block of  $\text{K}^+$  channels by imipramine may provide an explanation as to the occurrence of seizures and cardiac arrhythmias. Seizures, however, represent a complex phenomenon with a multifactorial aetiology. It is therefore conceivable that antidepressant-related seizures arise from a combination of mechanisms, mediated through a combination of short- and long-term interactions with multiple neurotransmitter and ion channel systems. Further study is warranted particularly in neurons expressing other  $\text{Na}^+$  channel subtypes found centrally such as  $\text{Na}_v1.2$  and  $\text{Na}_v1.3$  (Goldin, 2001), especially in view of the potential seriousness of seizures, and the extent of worldwide antidepressant drug usage.

## Acknowledgements

The authors wish to thank Dr. Max Willow for his help with the neurochemical experiments, Ms. Cathy Zappia (Department of Health Sciences, UTS) for assistance with the preparation of the rat brain synaptosomes and Dr. John Daly (National Institute of Diabetes and Digestive and Kidney Diseases, NIH, Bethesda, MD) for the gift of unlabelled batrachotoxin. Supported by a Clive and Vera Ramaciotti Foundation Grant and a UTS Internal Research Grant to G.M.N.

## References

- Arita, M., Wada, A., Takara, H., Izumi, F., 1987. Inhibition of  $^{22}\text{Na}^+$  influx by tricyclic and tetracyclic antidepressants and binding of [ $^3\text{H}$ ]imipramine in bovine adrenal medullary cells. *J. Pharmacol. Exp. Ther.* 243, 342–348.
- Baker, M., Bostock, H., Grafe, P., 1985. Accommodation in rat myelinated axons depends on two pharmacologically distinct types of potassium channels. *J. Physiol.* 369, 102.
- Benet, L.Z., Williams, R.L., 1990. Design and optimisation of dosage regimens; pharmacokinetic data. In: Gilman, A.G., Rall, T.W., Nies A.S., Taylor, P. (Eds.), *Goodman and Gilman's The Pharmacological Basis of Therapeutics*. Pergamon, Oxford, pp. 1650–1735.
- Bennett, M.R., Middleton, J., 1975. An electrophysiological analysis of the effects of amine-uptake blockers and  $\alpha$ -adrenoceptor blockers on adrenergic neuromuscular transmission. *Br. J. Pharmacol.* 55, 87–95.
- Bou-Abboud, E., Nattel, S., 1998. Molecular mechanisms of the reversal of imipramine-induced sodium channel blockade by alkalization in human cardiac myocytes. *Cardiovasc. Res.* 38, 395–404.
- Catterall, W.A., 1976. Purification of a toxic protein from scorpion venom which activates the action potential  $\text{Na}^+$  ionophore. *J. Biol. Chem.* 251, 5528–5536.
- Catterall, W.A., 1980. Neurotoxins that act on voltage-sensitive sodium channels in excitable membranes. *Ann. Rev. Pharmacol. Toxicol.* 20, 15–43.
- Cheng, Y., Prusoff, W., 1973. Relationship between inhibition constant ( $K_i$ ) and the concentration of an inhibitor which causes 50% inhibition ( $\text{IC}_{50}$ ) of an enzymatic reaction. *Biochem. Pharmacol.* 22, 3099–3108.
- Colquhoun, D., Hawkes, A.G., 1983. The principles of the stochastic interpretation of ion-channel mechanisms. In: Sakmann, B., Neher, E. (Eds.), *Single Channel Recording*. Plenum, New York, pp. 135–175.
- Delpón, E., Valenzuela, C., Tamargo, J., 1990. Tonic and frequency-de-

- pendent  $V_{\max}$  block induced by imipramine in guinea pig ventricular muscle fibers. *J. Cardiovasc. Pharmacol.* 15, 414–420.
- Delpón, E., Tamargo, J., Sanchez-Chapula, J., 1991. Further characterization of the effects of imipramine on plateau membrane currents in guinea-pig ventricular myocytes. *Naunyn-Schmiedeberg's Arch. Pharmacol.* 344, 645–652.
- Delpón, E., Tamargo, J., Sanchez-Chapula, J., 1992. Effects of imipramine on the transient outward current in rabbit atrial single cells. *Br. J. Pharmacol.* 106, 464–469.
- Fedulova, S.A., Vasilyev, D.V., Veselovsky, N.S., 1998. Voltage-operated potassium currents in the somatic membrane of rat dorsal root ganglion neurons: ontogenetic aspects. *Neuroscience* 85, 497–508.
- Felts, P.A., Yokoyama, S., Dib-Hajj, S., Black, J.A., Waxman, S.G., 1997. Sodium channel  $\alpha$ -subunit mRNAs I, II, III, NaG, Na6 and hNE (PN1): different expression patterns in developing rat nervous system. *Mol. Brain Res.* 45, 71–82.
- Glitzbach, R.K., Preskorn, S.H., 1982. Brain concentrations of tricyclic antidepressants: single-dose kinetics and relationship to plasma concentrations in chronically dosed rats. *Psychopharmacology* 78, 25–27.
- Goldin, A.L., 2001. Resurgence of sodium channel research. *Annu. Rev. Physiol.* 63, 871–894.
- Goldin, A.L., Barchi, R.L., Caldwell, J.H., Hofmann, F., Howe, J.R., Hunter, J.C., Kallen, R.G., Mandel, G., Meisler, M.H., Netter, Y.B., Noda, M., Tamkun, M.M., Waxman, S.G., Wood, J.N., Catterall, W.A., 2000. Nomenclature of voltage-gated sodium channels. *Neuron* 28, 365–368.
- Gordon, D., 1997. Sodium channels as targets for neurotoxins: mode of action and interaction of neurotoxins with receptor sites on sodium channels. In: Lazarowici, P., Gutman, Y. (Eds.), *Toxins and Signal Transduction. Cellular and Molecular Mechanisms of Toxin Action Series*, Harwood Press, Amsterdam, pp. 119–149.
- Grunnet, M., Jespersen, T., Angelo, K., Frokjaer-Jensen, C., Klaerke, D.A., Olesen, S.P., Jensen, B.S., 2001. Pharmacological modulation of SK3 channels. *Neuropharmacology* 40, 879–887.
- Hondeghem, L.M., Katzung, B.G., 1977. Time- and voltage-dependent interactions of antiarrhythmic drugs with cardiac sodium channels. *Biochim. Biophys. Acta* 472, 373–398.
- Lee, K., McKenna, F., Rowe, I.C., Ashford, M.L., 1997. The effects of neuroleptic and tricyclic compounds on BKCa channel activity in rat isolated cortical neurones. *Br. J. Pharmacol.* 121, 1810–1816.
- Little, M.J., Wilson, H., Zappia, C., Cestele, S., Tyler, M.I., Martin-Eauclaire, M.-F., Gordon, D., Nicholson, G.M., 1998a.  $\delta$ -Atracotoxins from Australian funnel-web spiders compete with scorpion  $\alpha$ -toxin binding on both rat brain and insect sodium channels. *FEBS Lett.* 439, 246–252.
- Little, M.J., Zappia, C., Gilles, N., Connor, M., Tyler, M.I., Martin-Eauclaire, M.-F., Gordon, D., Nicholson, G.M., 1998b.  $\delta$ -Atracotoxins from Australian funnel-web spiders compete with scorpion  $\alpha$ -toxin binding but differentially modulate alkaloid toxin activation of voltage-gated sodium channels. *J. Biol. Chem.* 273, 27076–27083.
- Nelson, S.R., Mantz, M.L., Maxwell, J.A., 1971. Use of specific gravity in the measurement of cerebral edema. *J. Appl. Physiol.* 30, 268–271.
- Nicholson, G.M., Willow, M., Howden, M.E.H., Narahashi, T., 1994. Modification of sodium channel gating and kinetics by versutoxin from the Australian funnel-web spider *Hadronyche versuta*. *Pflügers Arch. (Eur. J. Physiol.)* 428, 400–409.
- Ogata, N., Narahashi, T., 1989. Block of sodium channels by psychotropic drugs in single guinea pig cardiac myocytes. *Br. J. Pharmacol.* 97, 905–913.
- Ogata, N., Tatebayashi, H., 1989. Modulation of sodium current kinetics by chlorpromazine in freshly-isolated striatal neurones of the adult guinea-pig. *Br. J. Pharmacol.* 98, 1173–1184.
- Ogata, N., Tatebayashi, H., 1993. Differential inhibition of a transient  $K^+$  current by chlorpromazine and 4-aminopyridine in neurones of the rat dorsal root ganglia. *Br. J. Pharmacol.* 109, 1239–1246.
- Ogata, N., Nishimura, M., Narahashi, T., 1989a. Kinetics of chlorpromazine block of sodium channels in single guinea pig cardiac myocytes. *J. Pharmacol. Exp. Ther.* 248, 605–613.
- Ogata, N., Yoshii, M., Narahashi, T., 1989b. Psychotropic drugs block voltage-gated ion channels in neuroblastoma cells. *Brain Res.* 476, 140–144.
- Postma, S.W., Catterall, W.A., 1984. Inhibition of binding of [ $^3$ H]batrachotoxinin A 20- $\alpha$ -benzoate to sodium channels by local anesthetics. *Mol. Pharmacol.* 25, 219–227.
- Ragsdale, D.S., Scheuer, T., Catterall, W.A., 1991. Frequency and voltage-dependent inhibition of type IIA  $Na^+$  channels, expressed in a mammalian cell line, by local anesthetic, antiarrhythmic, and anticonvulsant drugs. *Mol. Pharmacol.* 40, 756–765.
- Ragsdale, D.S., McPhee, J.C., Scheuer, T., Catterall, W.A., 1996. Common molecular determinants of local anesthetic, antiarrhythmic, and anticonvulsant block of voltage-gated  $Na^+$  channels. *Proc. Natl. Acad. Sci. U. S. A.* 93, 9270–9275.
- Rash, L.D., Birinyi-Strachan, L.C., Nicholson, G.M., Hodgson, W.C., 2000. Neurotoxic activity of venom from the Australian eastern mouse spider (*Missulena bradleyi*) involves modulation of sodium channel gating. *Br. J. Pharmacol.* 130, 1817–1824.
- Richeimer, S.H., Bajwa, Z.H., Kahraman, S.S., Ransil, B.J., Warfield, C.A., 1997. Utilization patterns of tricyclic antidepressants in a multidisciplinary pain clinic: a survey. *Clin. J. Pain* 13, 324–329.
- Rosenstein, D.L., Nelson, J.C., Selby, C.J., 1993. Seizures associated with antidepressants: a review. *J. Clin. Psychiatry* 54, 289–299.
- Roy, M.L., Narahashi, T., 1992. Differential properties of tetrodotoxin-sensitive and tetrodotoxin-resistant sodium channels in rat dorsal root ganglion neurons. *J. Neurosci.* 12, 2104–2111.
- Safronov, B.V., Bischoff, U., Vogel, W., 1996. Single voltage-gated  $K^+$  channels and their functions in small dorsal root ganglion neurones of rat. *J. Physiol.* 493, 393–408.
- Stansfeld, C.E., Marsh, S.J., Halliwell, J.V., Brown, D.A., 1986. 4-Aminopyridine and dendrotoxin induce repetitive firing in rat visceral sensory neurones by blocking a slowly inactivating outward current. *Neurosci. Lett.* 64, 299–304.
- Trimble, M.R., 1980. New antidepressant drugs and the seizure threshold. *Neuropharmacology* 19, 1227–1228.
- Vaughan Williams, E.M., 1984. A classification of antiarrhythmic actions reassessed after a decade of new drugs. *J. Clin. Pharmacol.* 24, 129–147.
- Willow, M., Catterall, W.A., 1982. Inhibition of binding of [ $^3$ H] batrachotoxinin A 20- $\alpha$ -benzoate to sodium channels by the anticonvulsant drugs diphenylhydantoin and carbamazepine. *Mol. Pharmacol.* 22, 627–635.
- Willow, M., Gono, T., Catterall, W.A., 1985. Voltage-clamp analysis of the inhibitory actions of diphenylhydantoin and carbamazepine on voltage-sensitive sodium channels in neuroblastoma cells. *Mol. Pharmacol.* 27, 549–558.
- Wooltorton, J.R.A., Mathie, A., 1995. Potent block of potassium currents in rat isolated sympathetic neurones by the uncharged form of amitriptyline and related tricyclic compounds. *Br. J. Pharmacol.* 116, 2190–2200.